Penerbit Akademia Baru

Journal of Advanced Research in Fluid Mechanics and Thermal Sciences

Journal homepage: www.akademiabaru.com/arfmts.html
ISSN: 2289-7879

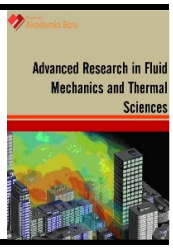

Influence of Heat Treatment on the Isothermal Oxidation of Fe-40Ni-24Cr Alloy

Open Access

Noraziana Parimin[1,*], Esah Hamzah[2], Astuty Amrin[3]

[1] School of Materials Engineering, Universiti Malaysia Perlis, 02600 Arau, Perlis, Malaysia
[2] Faculty of Mechanical Engineering, Universiti Teknologi Malaysia, 81310 Skudai Johor, Malaysia
[3] UTM Razak School of Engineering & Advanced Technology, UTM Kuala Lumpur, 54100 Kuala Lumpur, Malaysia

ARTICLE INFO

Article history:
Received 14 March 2018
Received in revised form 21 July 2018
Accepted 14 August 2018
Available online 2 September 2018

Keywords:
Isothermal oxidation, Fe-40Ni-24Cr alloy, heat treatment

ABSTRACT

The isothermal oxidation behaviour of two different heat treated of Fe-40Ni-24Cr alloy was studied in this work. The present paper focuses on the isothermal oxidation behaviour at 700ºC. Heat treatment at 2 different temperatures, namely 1000ºC and 1200ºC was applied to Fe-40Ni-24Cr alloy to alter the grain size of the samples. The heat treatment results showed that the average grain size increased with increase in heat treatment temperature. Optical microscopy, Scanning Electron Microscopy (SEM), Energy Dispersive X-Ray Spectroscopy (EDS) and X-Ray Diffraction (XRD) were employed in this study to analyse the oxidation behaviour of heat treated samples. The heat treated samples were subjected to oxidation experiment under isothermal conditions for 500 hours. The oxide scale formed during oxidation were generally complex consists of several oxide phases. The samples morphologies of oxidized samples were influenced by the alloy structure and expose conditions. The kinetics of oxidation followed the parabolic law which represent diffusion controlled oxide growth rate. Results indicate that the fine grain size of alloy heat treated at 1000ºC possess a better oxidation resistance and lowered the oxidation rate.

1. Introduction

Nickel (Ni)-based superalloys are used in nuclear reactors, electrical-resistance heaters, gas turbines, petrochemical, aerospace, and heat-treating industries, due to their favourable strength and excellent resistance to oxidation at elevated temperatures [1]. Ni-based superalloys has the ability to form protective surface oxide scales at high temperatures that provides them with resistance to further high temperature oxidation [1-2]. Based on its advantages, these alloys are widely used in many applications as high temperature structural materials. Fe-40Ni-24Cr (HR-120) alloy is a general purpose engineering material for applications that require resistance to heat and corrosion. The alloy is a solid-solution strengthened heat resistant alloy that provides excellent strength at elevated temperature.

* *Corresponding author.*
E-mail address: noraziana@unimap.edu.my (Noraziana Parimin)

Its oxidation resistance is comparable to other widely used Fe-Ni-Cr materials, such as alloys 330 and 800H [3]. Fe-40Ni-24Cr alloy was used in the petrochemical industries, typically contains a small amount of Nb and Ti as an alloying element [4–7]. This alloy are strengthened by carbides precipitation such as MC carbides composed of NbC, TiC and (Nb,Ti)C [8–14]. HR-120 alloy exhibits good resistance to oxidizing environments and can be used at temperatures up to 1205ºC. Under the aforementioned applications, Fe-40Ni-24Cr alloys encounter elevated temperatures, thermal cycling and/or long service life. In order to survive with severe environment applications, these alloys must develop a thermodynamically stable protective oxide layer with excellent resistance to oxide exfoliation. One way to mitigate oxide exfoliation is by refining the grain size of the alloy structure by means of heat treatment processes.

2. Methodology

The materials used in this study was commercial HAYNES HR-120 alloy, supplied by Haynes International, Inc., with the measured chemical composition (in wt%): 40.45 Ni, 24.11 Cr, 0.05 C, 0.08 Al, 0.03 Ti, 0.44 Si, 0.7 Mn, 0.01 P, 0.11 Cu, 0.25 Mo, 0.001 B, 0.17 Co, 0.44 Nb, 0.05 W and balance Fe.

A test sample was cubical coupons with nominal dimensions of 10 x 10 x 3 mm. The as-received alloy was subjected to heat treatment process at temperature of 1000°C and 1200°C for 3 hours followed by water quench. These samples are denoted as heat-treated 1000°C (HT1000) and heat-treated 1200°C (HT1200). The microstructure of heat-treated samples was characterized using optical microscopy. The grain size of heat-treated sample was measured using linear intercepts methods. The heat-treated samples were ground to P600 grit surface finish, cleaned with acetone and the dimension of the sample was measured. All samples were weight before and after the oxidation experiment to measure the weight changes using Metler AT400 analytical balance with sensitivity of 0.1 mg. The isothermal oxidation tests were investigated by means of discontinuous testing at 700°C up to 500 hours. The surface morphology of oxidized samples were characterized by Scanning Electron Microscopy (SEM) and Energy Dispersive X-Ray Spectroscopy (EDX). The phase analysis was identified using X-Ray Diffraction (XRD) technique.

3. Results and Discussion

3.1 Microstructure of Solution Annealed Samples

Figure 1 shows the optical micrographs of two heat-treated samples. The microstructure of all samples shows a matrix austenite phase. Results indicate that increasing in heat treatment temperature enlarge the sample grain size. HT1000 sample shows a fine grain size that is 29.46 µm meanwhile the HT1200 sample shows a coarser grain size that is 40.86 µm.

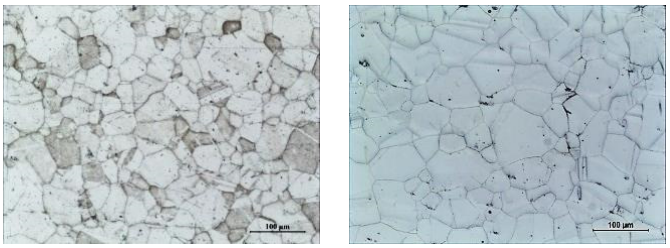

(a) HT1000 (b) HT1200

Fig. 1. Microstructure of heat-treated samples

3.2 Kinetic of Oxidation

Figure 2 illustrates the weight changes of the two heat-treated samples which are oxidized at 700°C for 500 hours. The curves indicate the trend of the weight gain as a function of exposure time for HT1000 and HT1200 samples, respectively. The oxidation kinetics of all samples followed parabolic rate law indicating the diffusion controlled oxide growth rate. As the oxide scale increase in thickness, the diffusion of ion species will slowly decrease, hence lowering the oxidation rate. The oxidation kinetic of fine grain HT1000 sample indicated a low oxidation rate with steady increasing in weight gain as the exposure time increases. The parabolic rate constant recorded a small value, which is 2.28 x 10^{-7} $mg^2cm^{-4}s^{-1}$.

In contrast, the high oxidation rate shows by coarse grain structure HT1200 sample. The weight gain of this sample indicates an increasing trend as the exposing duration increase. The parabolic rate constant for this sample is 7.29 x 10^{-7} $mg^2cm^{-4}s^{-1}$. The HT1200 sample recorded a high weight gain at the beginning, followed by a steady weight gain until 400 hours. After 400 hours of exposure, the oxidation rate showed a mild weight gain due to the possible occurrence of minor oxide spallation or oxide cracking which will be discussed later. The higher weight gain of HT1200 sample is due to the possible continuous oxide growth to develop a protective layer at the alloy surface.

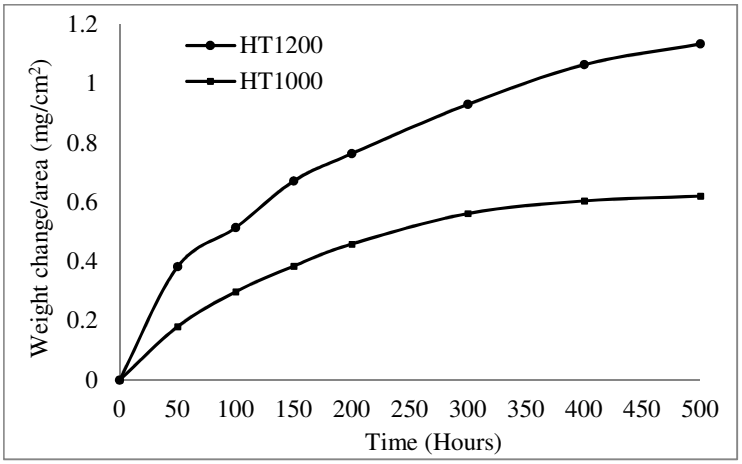

Fig. 2. Weight gain data for two heat-treated samples oxidized at 700ºC

3.3 Phase Analysis

Figure 3 shows the surface XRD patterns of the two heat-treated samples after exposure for 500 hours. The most intense austenite peaks represent the base alloy. The Cr-rich oxides was detected composes of several oxides which are Cr_2O_3, $Cr_{1.3}Fe0.7O_3$ and $(Cr_{0.88}Ti_{0.12})_2O_3$. In addition, less intense peaks of Ti-rich oxides also recorded composes of TiO_2 and $(Ti_{0.97}Cr_{0.03})O_2$. The formation of Cr-Ti oxide of $(Cr_{0.88}Ti_{0.12})_2O_3$ and Ti-rich oxides are said to mitigate the Cr evaporation effect of Cr_2O_3 due to the lower vapour pressure of Cr-Ti oxides [15].

In addition, the hematite phase of Fe_2O_3 also recorded on the analysis with several peaks overlaps with Cr-rich oxide. The formation of hematite phase also believed to have significant impact on oxide exfoliation resistance. According to other researchers [15-16], the formation of hematite would reduce the coefficient of thermal expansion (CTE) mismatch in between hematite and spinel oxides due to the similar CTE volume.

The spinel oxide phase also was detected on the alloy surface, overlapped on each other, which are $MnCr_2O_4$, $MnFe_2O_4$, $FeCr_2O_4$, $NiCr_2O_4$, and $NiFe_2O_4$ oxides. The formation of Mn-Cr spinel oxides phases may also enhance the oxide spallation resistance due to the incorporated of Mn into the Cr oxide which can lower the activity of Cr_2O_3 by the formation of $MnCr_2O_4$ oxide [17]. The formation of magnetite phase and NbO_2 oxide were also detected on the oxidized sample. Oxidized Fe-40Ni-24Cr alloy were formed several oxide phase which are Cr-rich, Fe-rich, Nb-rich and spinel oxides structure that contributes the most to the oxide formation due to rapid diffusion of these metal ion during high temperature exposure.

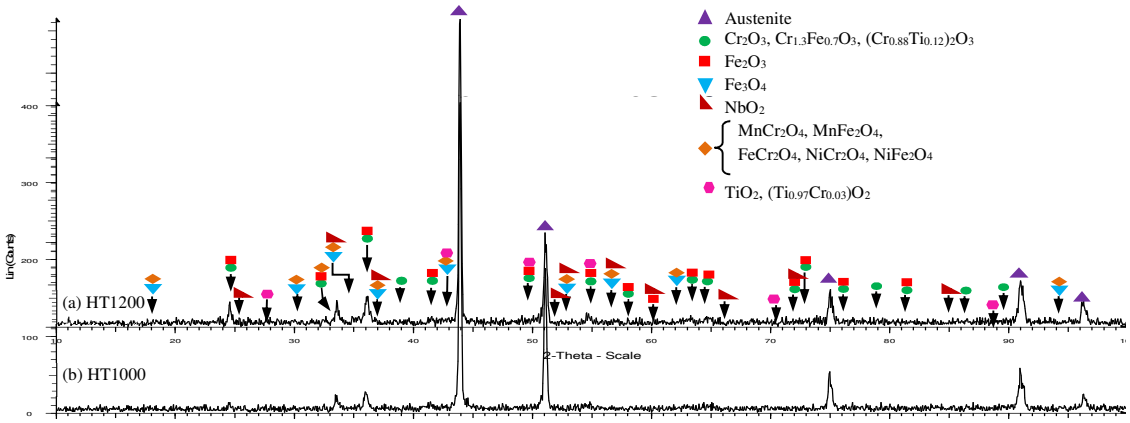

Fig. 3. XRD patterns of the oxidized

3.4 Surface Morphology of Oxidized Samples

Figure 4 (a) shows oxide morphology of HT1000 sample oxidized at 150 hours analysed with SEM corresponding secondary electron image (SEI). The oxide morphology of HT1000 sample indicates a serration oxide layer with EDX analysis at area B revealed an enrichment of elements O, Fe, Ni and Cr with less content of Mn. This analysis indicate the formation of several oxide phases on the sample surface. Figure 4 (b) shows an oxide morphology of HT1200 sample, indicated the distributed Nb-rich oxide particles with formation of isolated overgrown oxide on the sample.

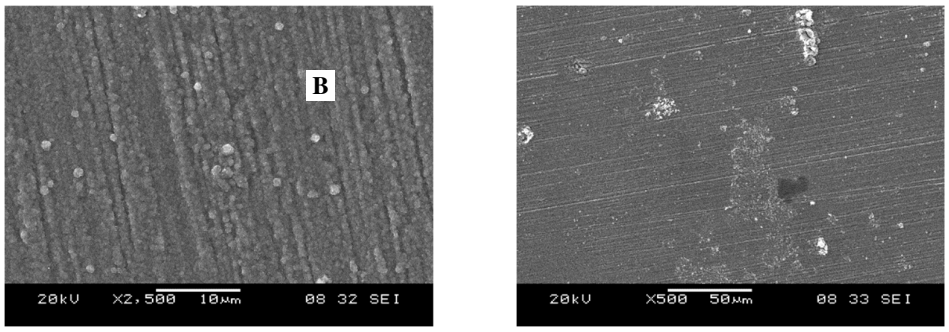

(a) HT1000 (b) HT1200

Fig. 4. SEM of Fe-40Ni-24Cr alloy isothermally oxidized at 700°C for 150 hours

Figure 5 shows oxide morphology of HT1000 sample oxidized at 300 hours analysed with SEM corresponding SEI. The image indicates that a uniform oxide layer with mild undulation and minor Nb-rich oxide particles distributed along the matrix area. Figure 6 (a) shows SEM image of HT1200 sample formed several oxide islands with distributed Nb-rich oxide particles on the oxidized surface.

Observation on high magnification (3000x) image (Figure 6 (b)) revealed a serration oxide layer formed on the matrix area, analyzed using EDX at C area, recorded a presence of elements O, Fe, Ni and Cr, with small content of Mn. Whereas, EDX analysis at the oxide island at D area, revealed the present of high amount of elements O and Cr, with slightly low content of elements Fe, Ni and Mn.

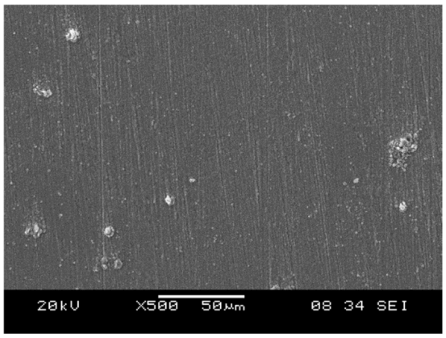

Fig. 5. SEM of HT1000 Fe-40Ni-24Cr alloy isothermally oxidized at 700ºC for 300 hours

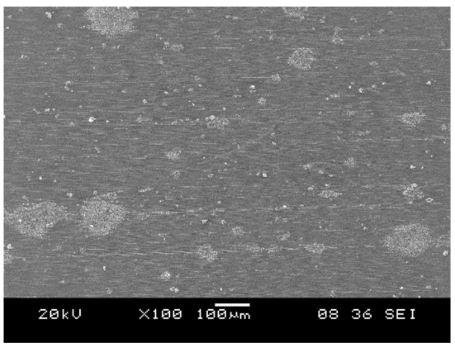

(a) 100x

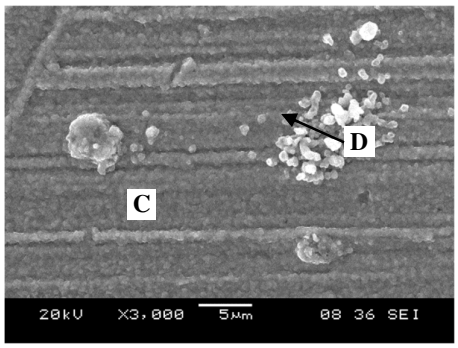

(b) 3000x

Fig. 6. SEM of HT1200 Fe-40Ni-24Cr alloy isothermally oxidized at 700ºC for 300 hours

Figure 7 shows oxide morphology of oxidized HT1000 samples for 500 hours. Low magnification (100x) of SEM image in Figure 7 (a) shows the presence of isolated oxide island and distributed of oxide particles at the alloy surface. The high magnification (1000x) image at the oxide island area demonstrated overgrew oxide particle was formed around Nb-rich oxide particles (Figure 7 (b)). The EDX analysis at area G indicates the enrichment of elements O, Cr and Nb, suggesting the formation of Cr and Nb rich oxide. Moreover, the high magnification image also recorded a spherical-like oxide particle which has different shape with Nb-rich oxide particles. The EDX analysis on this particle (H) revealed a higher content of elements O, Ti and Cr that probably compose of Cr-rich, Ti-rich and/or Cr/Ti-rich oxide.

Figure 8 shows oxide morphology of HT1200 samples of Fe-40Ni-24Cr alloy exposed at 700ºC for 500 hours. A low magnification (100x) image (Figure 8 (a)) of HT1200 sample showed the formation of several oxide islands which are displayed in high magnification image in Figure 8 (b), (c) and (d). The image in Figure 8 (b) showed a formation of Nb-rich oxide particle in the middle of the overgrown oxide island. Whereas, Figure 8 (c) showed the formation of oxide cracking on the overgrown oxide island with some oxide had been spall.

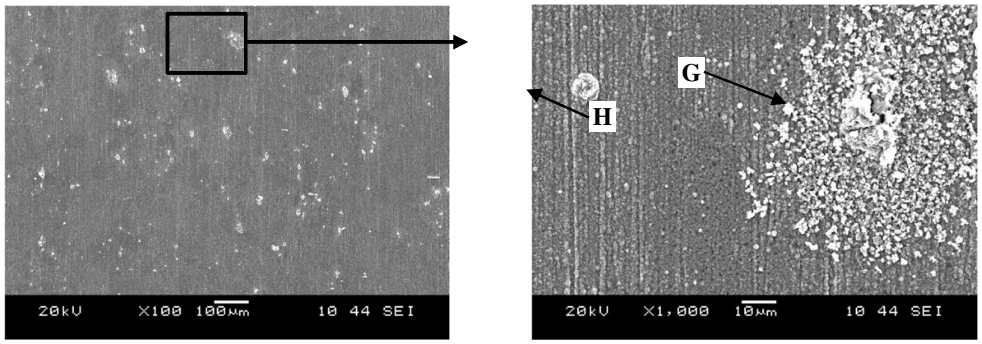

(a) 100x (b) 1000x

Fig. 7. SEM of HT1000 Fe-40Ni-24Cr alloy isothermally oxidized at 700ºC for 500 hours

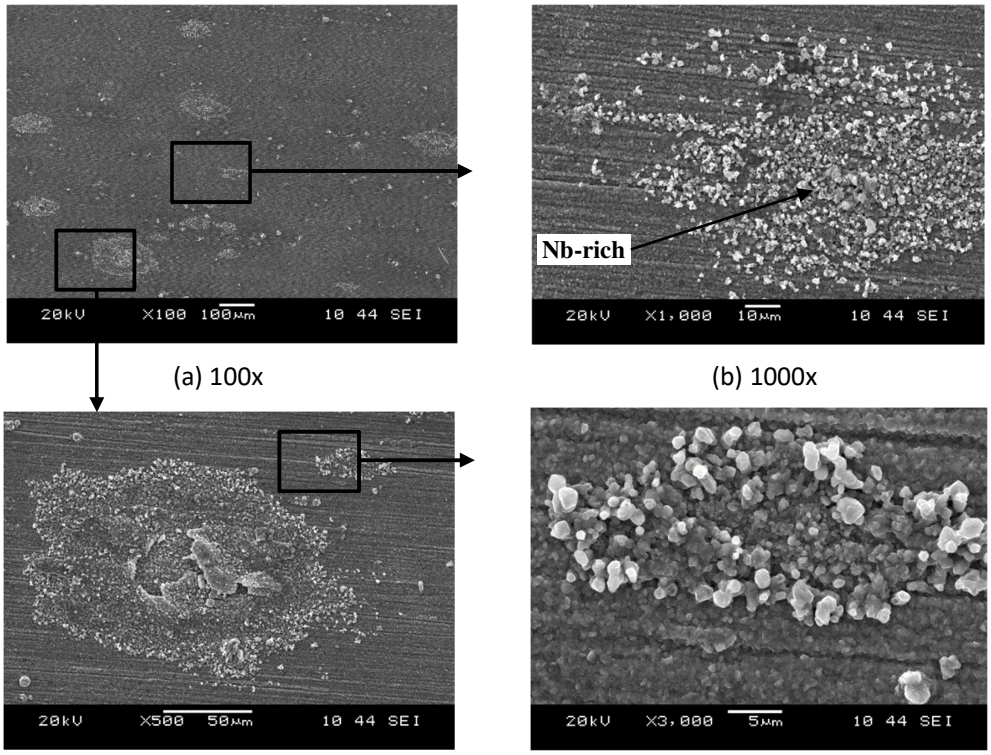

(a) 100x (b) 1000x

(c) 500x (d) 3000x

Fig. 8. SEM of HT1200 Fe-40Ni-24Cr alloy isothermally oxidized at 700ºC for 500 hours

Nb was added to the alloy system to improve the mechanical properties of the alloy. However, the Nb addition resulted in a large fraction of Nb-rich precipitates which encouraged the occurrences of pitting [5]. Therefore, the pitting may be associated with the Nb-rich precipitate which due to the massive compositional differences between the matrix and precipitate. The extensive growth of oxide scale tend to create the small difference in volume thermal expansion coefficients between the oxides and metals [15]. Cracks were induces the oxide to grow faster as it's develop the un-protective surface. This phenomenon will continuously happen until the stable protective oxide layer develops at the alloy surface. This feature was support the oxidation kinetics trend for HT1200 sample as discussed earlier that shows the mild weight gain at 400 hours exposure due to the minor oxide spallation induce by crack of overgrow oxides.

4. Conclusion

Heat treatment was applied to Fe-40Ni-24Cr alloy to alter the grain size of the alloy to improve protective oxidation behaviour. Heat-treated samples were oxidized at 700ºC for 500 hours. It was found that the fine and coarse grain size was produced by the heat treatment on Fe-40Ni-24Cr alloys. The oxidation of all samples tends to follow the parabolic rate law. The oxidation rate of the fine grain (HT1000) was slower compared to the coarse grain (HT1200). HT1000 exhibited the lowest weight gain hence the superior oxidation resistance. The morphological surfaces of the HT1200 samples indicate an oxide spallation on the oxide scale surface resulting in the high oxidation rate.

Acknowledgments

The authors would like to thank the Ministry of Higher Education Malaysia for the research fund under the Fundamental Research Grant Scheme (FRGS) (Project Code. FRGS/1/2016/TK05/UNIMAP/02/4).

References

[1] Barnard, B. R., P. K. Liaw, R. a. Buchanan, and D. L. Klarstrom. "Affects of applied stresses on the isothermal and cyclic high-temperature oxidation behavior of superalloys." *Materials Science and Engineering: A 527*, no. 16–17 (2010): 3813–3821.

[2] Fulger, M., D. Ohai, M. Mihalache, M. Pantiru, and V. Malinovschi. "Oxidation behavior of Incoloy 800 under simulated supercritical water conditions." *Journal of Nuclear Materials* 385, no. 2 (2009): 288–293.

[3] HAYNESS International. "HAYNES ® HR-120 TM alloy." (H-2135D). U.S.A: Haynes International (2008).

[4] Tari, V., a. Najafizadeh, M. H. Aghaei, and M. a. Mazloumi. "Failure Analysis of Ethylene Cracking Tube." *Journal of Failure Analysis and Prevention* 9, no. 4 (2009): 316–322.

[5] Tan, L., X. Ren, K. Sridharan, and T. R. Allen. "Corrosion behavior of Ni-base alloys for advanced high temperature water-cooled nuclear plants." *Corrosion Science* 50, no. 11 (2008): 3056–3062.

[6] Ray, A. K., S. K. Sinha, Y. N. Tiwari, J. Swaminathan, G. Das, S. Chaudhuri, and R. Singh. "Analysis of failed reformer tubes." *Engineering Failure* Analysis 10, no. 3 (2003): 351–362.

[7] Kaya, A. A., P. Krauklis, and D. J. Young. "Microstructure of HK40 alloy after high temperature service in oxidizing / carburizing environment I. Oxidation Phenomena and Propagation of a crack." *Materials Characterization* 49 (2002): 11–21.

[8] Sustaita-Torres, I. a., S. Haro-Rodríguez, M. P. Guerrero-Mata, M. de la Garza, E. Valdés, F. Deschaux-Beaume, and R. Colás. "Aging of a cast 35Cr–45Ni heat resistant alloy." *Materials Chemistry and Physics* 133, no. 2–3 (2012): 1018–1023.

[9] Borjali, S., S. R. Allahkaram, and H. Khosravi. "Effects of working temperature and carbon diffusion on the microstructure of high pressure heat-resistant stainless steel tubes used in pyrolysis furnaces during service condition." *Materials & Design* 34 (2012): 65–73.

[10] Piekarski, B. "The influence of Nb, Ti, and Si additions on the liquidus and solidus temperatures and primary microstructure refinement in 0.3C-30Ni-18Cr cast steel." *Materials Characterization* 61, no. 9 (2010): 899–906.

[11] Dehmolaei, R., M. Shamanian, and a. Kermanpur. "Microstructural characterization of dissimilar welds between alloy 800 and HP heat-resistant steel." *Materials Characterization* 59, no. 10 (2008): 1447–1454.

[12] Ribeiro, A. F., L. H. De Almeida, D. Fruchart, and G. S. Bobrovnitchii. "Microstructural modifications induced by hydrogen in a heat resistant steel type HP-45 with Nb and Ti additions." *Journal of Alloys and Compounds* 357 (2003): 693–696.

[13] de Almeida, L. H., A. F. Ribeiro, and I. Le May. "Microstructural characterization of modified 25Cr–35Ni centrifugally cast steel furnace tubes." *Materials Characterization* 49, no. 3 (2002): 219–229.

[14] Piekarski, B. "Effect of Nb and Ti additions on microstructure, and identification of precipitates in stabilized Ni-Cr cast austenitic steels." *Materials Characterization* 47, no. 3–4 (2001): 181–186.

[15] Tan, L., X. Ren, K. Sridharan, and T. R. Allen. "Effect of shot-peening on the oxidation of alloy 800H exposed to supercritical water and cyclic oxidation." *Corrosion Science* 50, no. 7 (2008): 2040–2046.

[16] Tan, L., K. Sridharan, and T. R. Allen. "The effect of grain boundary engineering on the oxidation behavior of INCOLOY alloy 800H in supercritical water." *Journal of Nuclear Materials* 348, no. 3 (2006): 263–271.

[17] Zurek, J., D. J. Young, E. Essuman, M. Hänsel, J. J. Penkalla, L. Niewolak, and W. J. Quadakkers. "Growth and Adherence of Chromia Based Surface Scales on Ni-Base Alloys in High- and Low-pO2 Gases." *Materials Science and Engineering: A 477*, no. 1-2 (2008): 259–270.